# Enhancement Of Cell And Chromosome Images Using Optimized Filter Masks In Fourier Transformed Space

Hutzler, P.

P. J.S. Hutzler, "Enhancement Of Cell And Chromosome Images Using Optimized Filter Masks In Fourier Transformed Space," Proc. SPIE 0515, Medical Images and Icons, (3 August 1984); doi: 10.1117/12.964800

Event: Medical Images and Icons, 1984, Arlington, United States

ENHANCEMENT OF CELL AND CHROMOSOME IMAGES
USING OPTIMIZED FILTER MASKS IN FOURIER TRANSFORMED SPACE

P.J.S. HUTZLER

GSF-Abteilung für Angewandte Optik
D-8042 Neuherberg, West-Germany

Abstract

Image processing by linear systems has some fascinating aspects due to the theorems of the Fourier transform (FT). Those, whose FT operator is a piece of glass are quite familiar to them, thinking in object space images and FT space images by reason of visual experience. But also in digital image processing the study of FT images is advantageous, e.g. when designing linear filters. The realization of an apodized Laplacian operator is shown, using an image of G-banded chromosomes as test objects. The quality of the filters is tested by the application of a contour-algorithm onto the filtered images.

Introduction

The convolution theorem of linear systems tell us that the convolution of two functions, and the Fourier transform of the product of their transforms give the same result[1].

$$\int_{-\infty}^{+\infty} f(u)g(\mathbf{x}-u)du = \int_{-\infty}^{+\infty} F(s)G(s)\exp[i2\pi\mathbf{xs}]\, ds \qquad (1a)$$

where $F(\mathbf{s}) = \int_{-\infty}^{+\infty} f(\mathbf{x})\exp[-i2\pi\mathbf{xs}]\, \mathbf{dx}$ and $\mathbf{x} = \{x,y\}$

When $G(\mathbf{s})$ is the transfer function of the linear system then its transform $g(\mathbf{x})$ is the system impulse response. Although both sides of equation (1) yield the same result, their practical realizations in digital image processing show quite different aspects. For instance, convolution is fast as far as the impuls response matrices are small, but it becomes slower with increasing matrices, whereas the performance of the FT is independent of the filter.

Assuming a digitized image IM(x,y), a transfer function T(x,y), and a complex Fast Fourier Transform algorithm (FFT)[2], then the right hand side of (1a) is given by

$$IM_{out}(x,y) = FFT^{-1}\ T(u,v)\ \ FFT\ IM_{in}(x,y) \qquad (1b)$$

The Laplacian operator

The Laplacian operator has been suggested as an aid in luminescence threshold detection[3]. In two dimensions the operator takes the form

$$\nabla^2 f(x,y) = \left(\frac{\partial^2}{\partial x^2} + \frac{\partial^2}{\partial y^2}\right) f(x,y) \text{ at object space} \qquad (2a)$$

The application of the derivative theorem of Fourier transforms, which says:

$$FT\left[\frac{\partial}{\partial x} f(x,y)\right] = i2\pi uF(u,v), \text{ results in} \qquad (2b)$$

$$FT\left[\left(\frac{\partial^2}{\partial x^2} + \frac{\partial^2}{\partial y^2}\right) f(x,y)\right] = -4\pi^2 \cdot (u^2+v^2)F(u,v), \qquad (2c)$$

which is the FT version of the Laplacian.

The application of (2c) on digitized images of quadratic shape points out, that it emphasizes too much the high frequenices, especially at the corner regions. It rather works as a noice amplifier, than contour enhancing. Therefore a frequency limitation is introduced by means of an apodizing filter of Gaussian shape. The modified unsigned and apodized Laplacian tranfer function takes the form

$$T_{LP}(u,v) = N(u^2+v^2)\exp[-\pi(u^2+v^2)/a^2] \qquad (3)$$

where a gives the frequency limitation and N the amplitude normalization.



CH2047-9/84/0000/0433$01.00©1984 IEEE

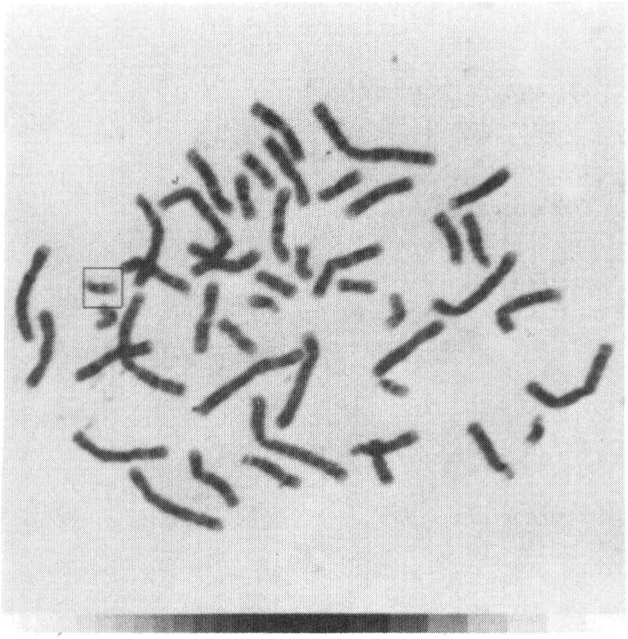

a) Original image, metaphase with G-banded chrom.

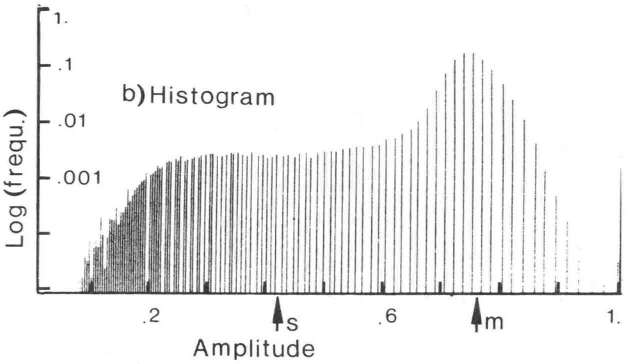


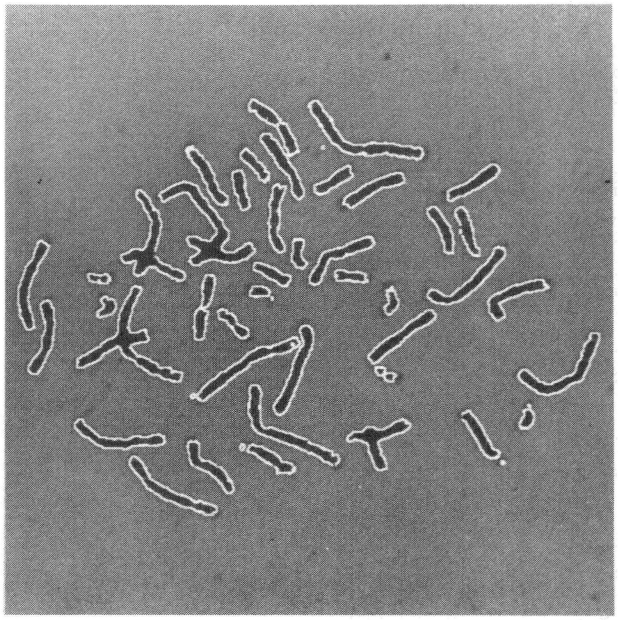

**Fig 1.** c) Original image with contours at 0.42

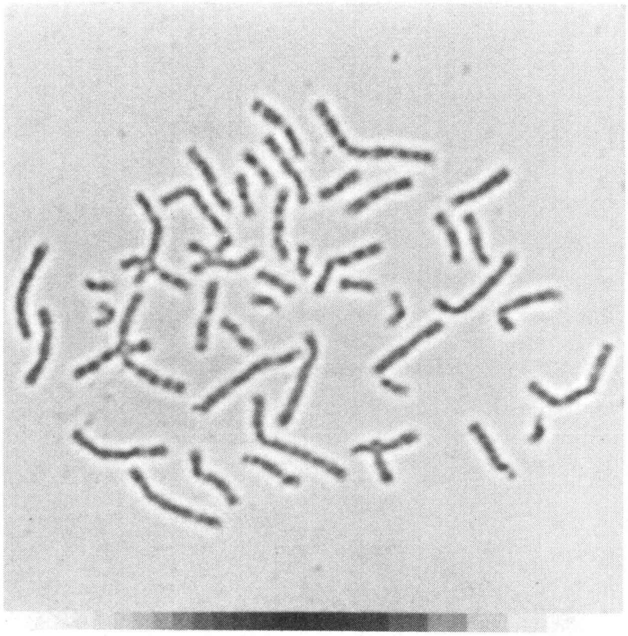

a) Image filtered with $T_{LP1}$

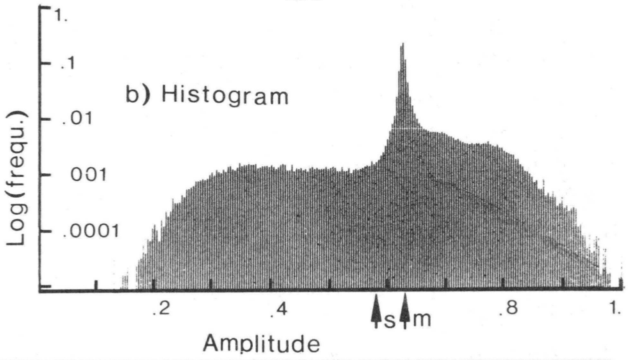


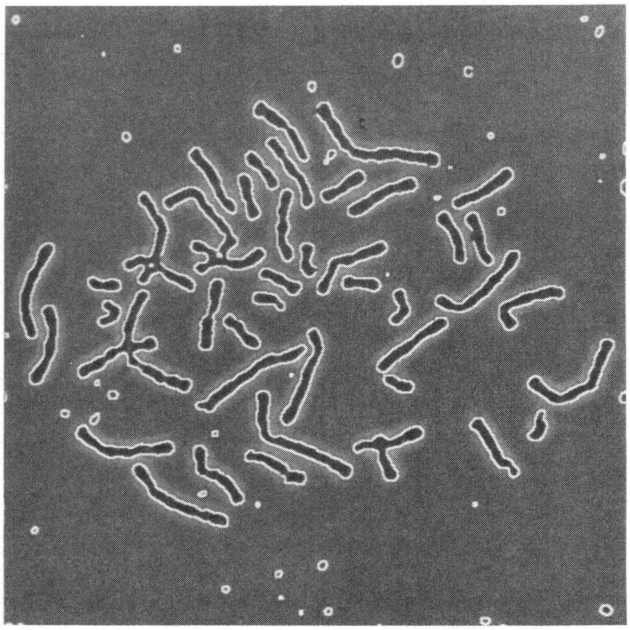

**Fig 2.** c) Image filtered with $T_{LP1}$ contours at s=0.58

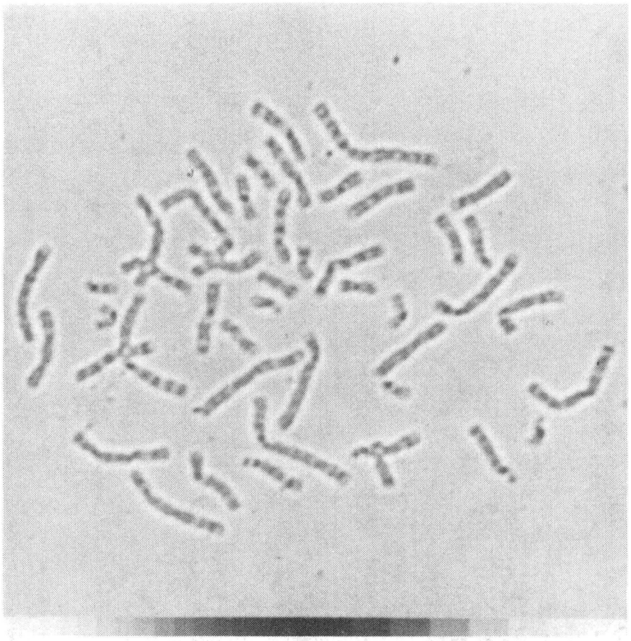

a) Image filtered with $T_{LP2}$

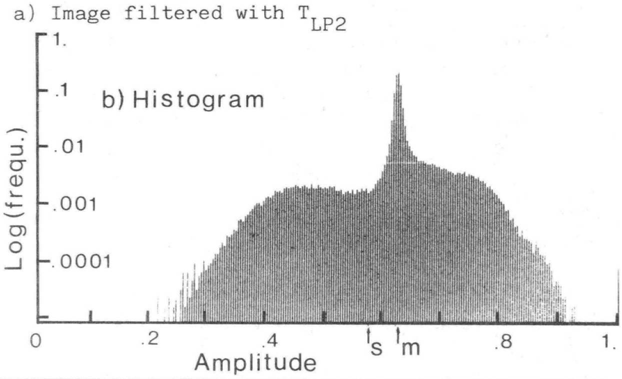


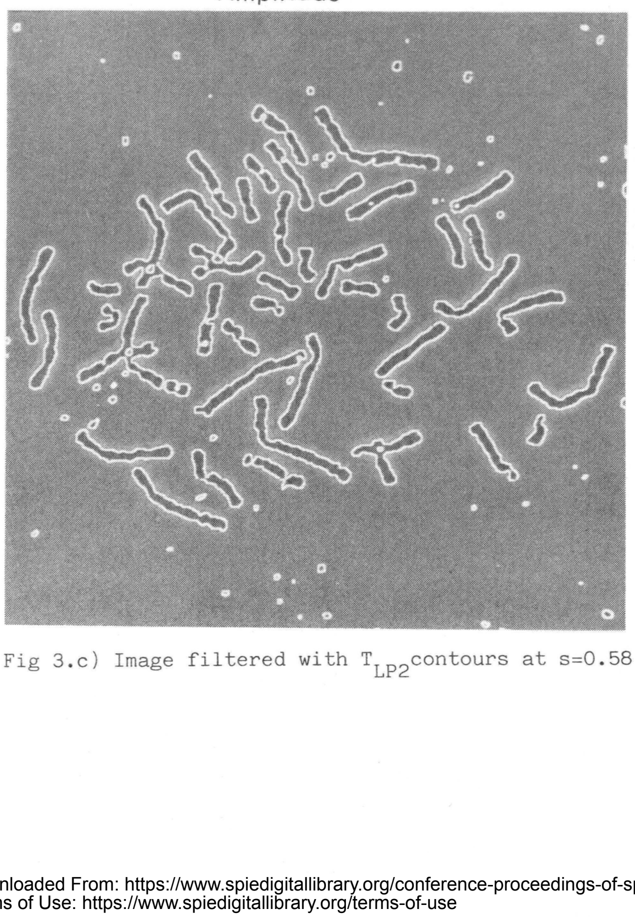

Fig 3.c) Image filtered with $T_{LP2}$contours at s=0.58

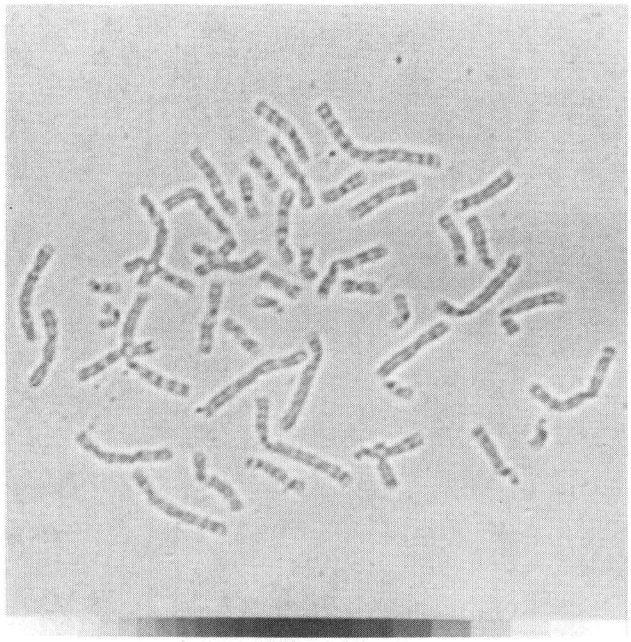

a) Image filtered with $T_{LP3}$

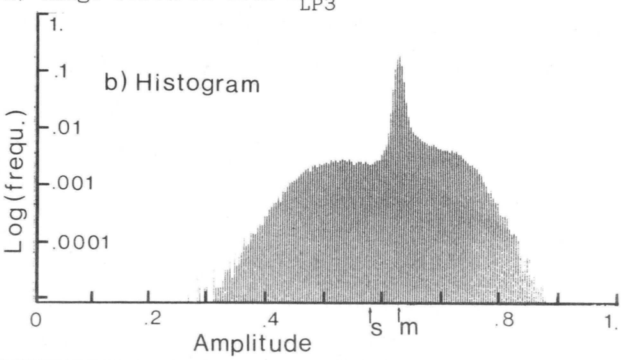


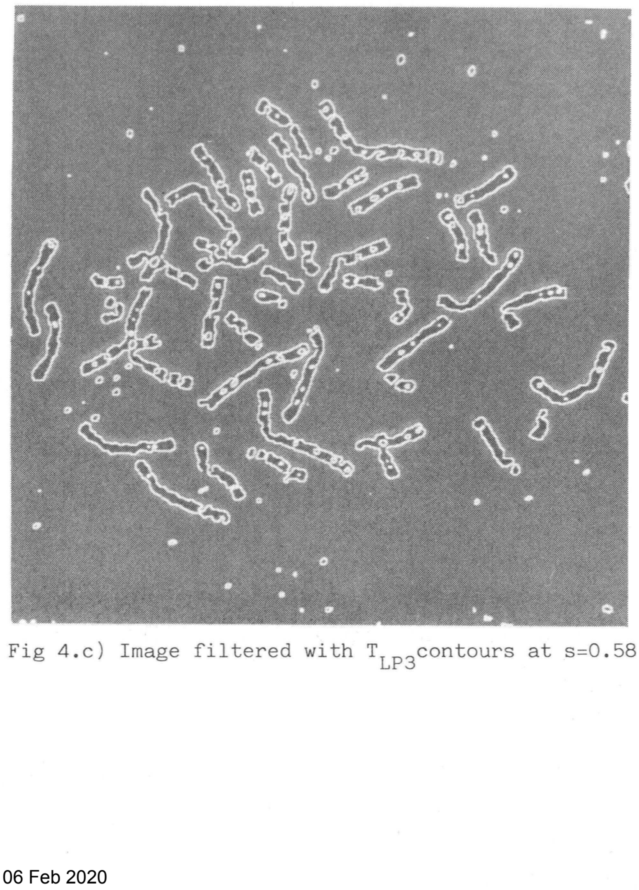

Fig 4.c) Image filtered with $T_{LP3}$contours at s=0.58

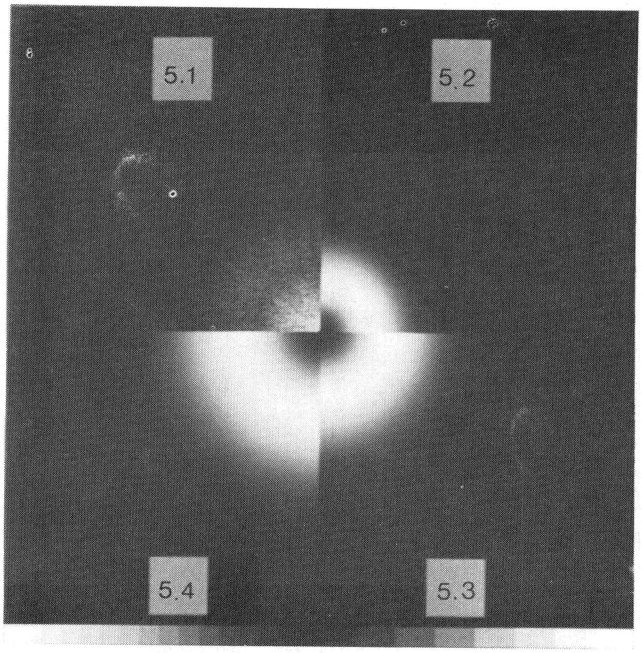


**Fig 5** Power spectrum of the mitotic cell (5.1) and the transfer function of the three Laplacian filters $T_{LP1}$(5.2), $T_{LP2}$(5.3), $T_{LP3}$(5.4).

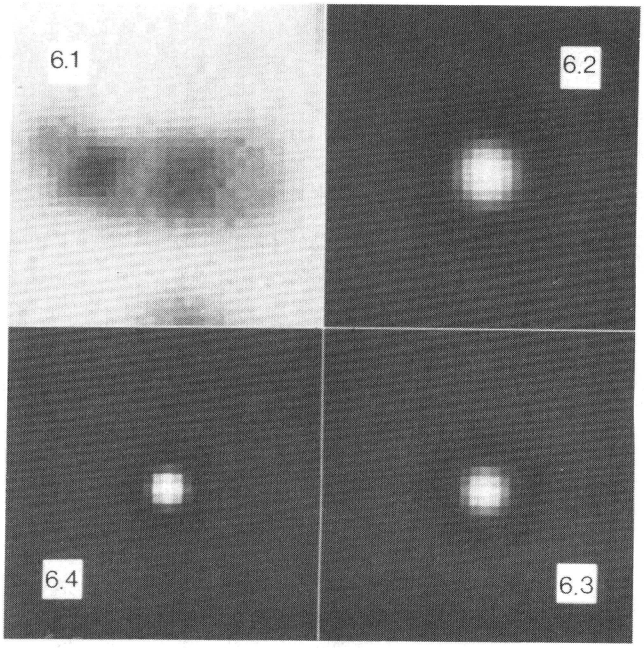


**Fig 6** Impulse response function of the three transfer functions at fig. 5. obtained by (4). One chromosome (6.1) for reference of size (32 x 32 pixels each quadrant).

Application of Filters

The image of a mitotic human cell treated with G-banding stain is used for demonstration (fig.1a) It is uniformly sampled to 512 x 512 pixels, each of them with 8 bit grey scale quantization. This, and all other images are taken from the digital image storing system's display monitor.

The Fourier transformed image is obtained by complex FFT. Fig. 5.1 displays the absolute values of it in logarithmic scale for one segment of the FT plane. Besides some speckling the FT image shows a characteristic radial signal distribution. There is a local minimum of the signal at a radius of about 53 pixels (linear matrix size is 512) which is followed by a maximum at a radius of 68 pixels. This min-max effect is induced by the chromosome internal banding structure and does not depend on the relative distance of the chromosomes[4]. There seems to be no relevant object information outside a radius of about 128, what is half of the total frequency range. Using equation (3) three different filter masks are calculated.

The two parameters N and a are chosen thus, that the transmittance varies between zero and one in each case, and the three masks have their maximum of transmittance at a radius of 39, 53 and 68 pixels in the frequency plane. One sector of each is displayed at figs. 5.2 to 5.4. A comparison with the object power spectrum at 5.1 shows that the most extended transfer function 5.4 covers the whole high frequency range of the object information but suppresses at lot of low frequency information. Whereas the smallest mask reduces the high frequency resolution considerably.

In accordance to

$$\text{Impulse response} = \text{FFT (transfer function)} \quad (4)$$

to three corresponding impulse responses were calculated. Due to the symmetry of the transfer function the impulse responses are real, too. But they have positive and negative values. The three impulse responses are displayed at an enlarged scale with 32 x 32 pixels each at figs. 6.2 to 6.4.

To display the negative values the signals have an offset of 16 within a range of 255 grey levels.

Equation (1b) was realized and applied to the input image (fig. 1a) using the three different transfer functions (figs. 5.2 to 5.4). The symmetry of the filter masks gives rise to real values in the output images. The resulting images are identically compressed to a dynamic range of 256 grey values, and displayed at figs. 2.a to 4.a. Figs. 1.b to 4.b show the histograms of the 4 images. The original image (fig. 1.a) is characterized by a broad maximum at relative signal amplitude m= 0.76. The broad shoulder left of it indicates a good dynamic range of the object signals. Missing grey levels are due to a shading correction procedure a registration time. The three images resulting from the linear filter operation show narrow maxima in their histograms at amplitude value zero (m = 0.63 in histogram scaling). A small shoulder right of the maxima at positiv signal range is caused by the overshoot resulting from differentiation. The histograms figs. 2.b to 4.b also indicate a drecreasing dynamic range of the object signals a negative value range, left of the maxima.

The narrow maxima in the histograms of the filtered images result from a relatively constant background signal this should be a good pre-condition for object separation. A simple contour algorithm linking locations with constant threshold value s was run over all images.

The results of the contouring procedure are displayed at figs. 1.c to 4.c. At the original image the threshold was taken just as low as necessary for obtaining a full separation of all chromosomes. At a threshold s = 0.42, what is the middle of the dynamic range of the objects, this separation was possible. At this level scarcely 'noise' particles are contoured, but several chromosomes are truncated, especially those ending with weak structure, and some chromosomes are just cut.

For all filtered images a threshold s = 0.58 just at the negative amplitude side of the maximum peak was chosen.

It turns out that at the image (fig. 1) obtained by application of filter $T_{LP1}$ chromosomes are neither truncated nor cut. The contours give a good reproduction of the object shape. However at figs. 3 and 4 the internal structure of the chromosomes becomes dominant in the contouring image.

The transfer function giving rise to the best contouring result is displayed at fig. 5.2 and the corresponding impulse response at fig. 6.2. Fig. 6.2 shows that the correlation mask giving (due to equation 1.a) the results of fig. 2 needs at least a linear matrix size of 15. Correlation masks which can be realized within a smaller linear matrix size like thoseat figs. 6.3 and 6.4 would result in contours worse than using the original image.

<u>References:</u>


1. R. Bracewell, The Fourier Transform and its Application (McGraw-Hill, New York, 1965)
2. D. Fraser, Optimized Mass Strage FFT Program, in Programs for Digital Signal Processing (Ed. Digital Signal Processing Committee, IEEE Press, New York, 1979)
3. W.K. Pratt, Digital Image Processing (John Wiley & Sons, New York, 1978)
4. P.J.S. Hutzler, Applied Optics <u>23</u>, 776 (1984)